Hindawi
Geofluids
Volume 2022, Article ID 3575541, 9 pages
https://doi.org/10.1155/2022/3575541

Research Article

Experimental Study on the Variation of Soil Dielectric Permittivity under the Influence of Soil Compaction and Water Content

Jun Hu,[1] **Xinbin Wang**,[2] **Fujun Zhang**,[3] **and Yuanke Zhao**[1]

[1]*Gansu Provincial Transportation Research Institute Group Co., Ltd, Lanzhou 730000, China*
[2]*Northwest Institute of Eco-Environment and Resources, Lanzhou 730000, China*
[3]*Gansu Changda Highway Co., Ltd, Lanzhou 730000, China*

Correspondence should be addressed to Xinbin Wang; wangxinbin@lzb.ac.cn

Received 18 May 2022; Accepted 16 September 2022; Published 18 November 2022

Academic Editor: Nicoló Colombani

The dielectric permittivity of common soils is mainly controlled by water content and porosity, while the latter is closely related to the characteristics of compaction. By studying the changes in dielectric permittivity of soil samples with different soil water content and compaction levels, the influence of the controlling factors on the relationship model between soil water content and dielectric permittivity can be evaluated. In this paper, network analyzer was used to measure the dielectric permittivity of 7 groups of soil samples with gravimetric water content ranging from 8.09% to 14.52% and dry density ranging from 1.61 g/cm^3 to 1.96 g/cm^3. The results show that the dielectric permittivity increases with the increase of water content and dry density, and the effect of water content on permittivity is more significant for soils with higher dry density. Furthermore, when the water content is less than or equal to the optimal water content, Topp formula and the complex refractive index model (CRIM) can better predict the soil dry density. When the water content approaches the saturated state of soil, there is a deviation between the predicted value and the actual value. At last, the modified Topp formula and the complex refractive index model (CRIM) can accurately predict soil compactness. This provides an important basis for rapid detection of water content and compactness of highway subgrade soil by ground penetrating radar.

1. Introduction

The dielectric permittivity is a physical parameter that characterizes dielectric properties or polarization properties of dielectric materials. Dielectric permittivity of rock and soil media is a basic parameter of remote sensing and geophysical technology [1, 2]. The dielectric permittivity of rock and soil, as well as their mechanical properties, are influenced by water content and porosity, while the porosity of soil and rock is closely related to compaction characteristics [3–8].

Different relational models of dielectric permittivity and water content apply to the dielectric permittivity tested in the frequency range from 100 MHz to 10 GHz. In the low-frequency band, the intensification mechanism causes the dielectric permittivity of rocks and soils to increase with decreasing frequency, and in the high frequency band (higher than 10 GHz), the dielectric permittivity values start to decrease as they start to approach the relaxation frequency of water molecules [9], the dielectric permittivity value in the high frequency band is the dielectric permittivity value used in the different relational models [10].

Since the dielectric permittivity value of water in the high-frequency band is about 80, which is much higher than the dielectric permittivity value of solid particles (dielectric permittivity value is about 4) and air (dielectric permittivity value is equal to 1) [11], the dielectric permittivity response of rocks and soils is sensitive to the water content. Secondary factors affecting the dielectric permittivity response of soils

and rocks include the effective properties of pores and solid particles, and small-scale laminar structure, temperature, and the salt content of soil and rock solutions.

Numerous relational models have been used to describe the relationship between the soil dielectric permittivity with its constituents [12], volume percentage and water content [13], such as the Cole-Cole and Cole-Davidson dielectric permittivity models, the Topp Equation [14], Refractive Index (RI) Model, and the complex refractive index model (CRIM) [15–17].

The most widely used relational models are TOPP formula and CRIM model [18, 19]. However, the relational model to describe the different types of soil dielectric permittivity and the moisture content (such as TOPP formula) or the soil dielectric permittivity and the soil composition, dielectric permittivity volume content of each part (such as CRIM formula), the relationship between the porosity of the soil rock and particle size of high frequency dielectric permittivity response model has yet to see the influence of related research, TOPP formula and CRIM formula also need to be corrected or verified according to different use environments to improve the accuracy of quantitative interpretation.

Therefore, through dielectric permittivity tests of soil samples with different soil water content and porosity (compaction level), the paper intends to study the influence of the dielectric permittivity value of soil with different compaction levels, and the feasibility of studying soil compaction level through dielectric permittivity test, as well as the relationship between soil compaction level and its dielectric permittivity. The research results will provide an important theoretical basis and data support for the detection of water content and compaction level of highway subgrade soil at construction sites.

2. Sample Preparation

To study the relational model of soil water content, compaction level, and other factors on its dielectric permittivity value, the experiments prepared remolded samples with the same water content and different dry densities (porosity), and with different water contents and the same (similar) dry density (porosity) for dielectric permittivity test, respectively.

According to the test plan, the soils of the same type were first dried, ground, and sieved. Then cylindrical samples of the same volume were made in standard sample-making boxes of 10 cm diameter according to different densities and water contents. Each sample was encapsulated in cling film after configuration and left to stand for use.

The diameter of each sample is 61.80 mm. The mass water contents of experimental samples were 8.09%, 9.26%, 10.49%, 11.46%, 12.22%, 13.77%, and 14.52%, respectively. Each sample was applied with different sample preparation pressure to obtain soil samples with different dry densities, which corresponded to dry density variations in the ranges of 1.65-1.96 g/cm^3, 1.64-1.93 g/cm cm^3, 1.61-1.92 g/cm^3, 1.65-1.96 g/cm^3, 1.64-1.94 g/cm^3, 1.73-1.91 g/cm^3, and 1.75-1.88 g/cm^3, respectively.

Two identical soil samples were prepared to corresponding to each sample of the water content and compaction level for dielectric permittivity testing to reduce the random errors due to the sample preparation and dielectric permittivity testing process. Since the test area of the dielectric permittivity test probe is smaller than the sample size, to reduce the errors caused by the heterogeneity in the sample preparation process, multiple tests were performed on two planes of the same cylindrical sample, and a total of 10 measurements were performed for each sample. The sample geometry size, sample mass, dry density, and pressure used for samples prepared are shown in Table 1.

3. Equipment and Methods for Dielectric Permittivity Test

3.1. Equipment for Tests. The experiment used an ENA series E5061B microwave network analyzer produced by Agilent Technologies, Inc., with a frequency range from 100 KHz to 1.5 GHz, with electronic calibration parts and a probe software toolkit (Figure 1).

The microwave network analyzer has a signal source and receiver, can be transmitted through the signal source inside the instrument of different frequencies of electromagnetic waves, through the transmission line and the probe to the contact surface of the probe, and the tested material. After the interaction of electromagnetic waves and the tested material, part of the electromagnetic wave energy is lost. Another part of the energy is reflected, expressed by the reflection coefficient (S11), transmitted back by the transmission line, and recorded by the instrument's receiver. The S11 parameter can be converted into the real and imaginary parts of the dielectric permittivity by the device software and displayed on the instrument.

3.2. Instrument Calibration. The probe and console were placed in the environment and calibrated at the appropriate time after the instrument was started, first using the electronic calibration parts to calibrate network analyzer. Then, the calibration of the probe within the software was performed in 3 steps: first the probe was exposed to air for air calibration; then, a short circuit breaker was used to do the short-circuit calibration for the probe; and finally, the probe was calibrated with deionized water at 25°C. After the 3 calibrations were completed, validation measurements were performed on substances with known dielectric permittivity such as air and water, and only after the measurement data were qualified can the measurement process be forwarded to the actual sample. Otherwise the instrument must be recalibrated.

3.3. Measurement of Samples. After the network analyzer was calibrated, the prepared soil sample was fixed on a flat surface. The sample was measured using a coaxial plate probe, its dielectric permittivity was measured at the center and the edges, respectively, each point was measured no less than three times and the average value was taken, and the final result obtained can be considered as the dielectric permittivity value of this sample (Figure 2).

Table 1: Soil sample experimental parameters range.

Sample No.	Water content (%)	Sample height (mm)	Sample mass (g)	Dry density (g/cm^3)	Pressure (KN)
1	8.09	41.5 ~ 42.3	222.02~263.37	1.65~1.96	2.5 ~ 24.7
2	9.26	41.5 ~ 42.4	224.8 ~ 262.32	1.64~1.93	2.87~25.1
3	10.49	41.0 ~ 41.7	222.6 ~ 264.8	1.61~1.92	2.34~23.3
4	11.46	40.8 ~ 41.0	226.3 ~267.0	1.65~1.96	2.7 ~ 25.96
5	12.22	40.2 ~ 41.0	226.23~267.0	1.64~1.94	2.56~20.05
6	13.77	37.5 ~ 40.7	223.4 ~ 265.0	1.73~1.91	2.17~22.5
7	14.52	37.5 ~ 41.6	224.9 ~ 268.67	1.75~1.88	2.22~21.8

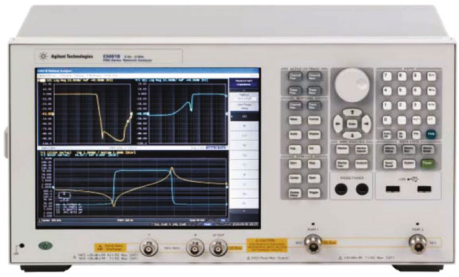

Figure 1: E5061B Network analyzer.

Figure 2: Dielectric permittivity testing.

4. Data Processing and Analysis

4.1. Repeat Tests of the Same Sample Dielectric Permittivity. The accurate measurement of the dielectric permittivity characteristics of a sample is the basis for subsequent processing and computational analysis. The dielectric permittivity tests on different parts of the same sample can evaluate the accuracy of the test results, the spatial variability of the sample water content, porosity, etc., and reduce the random errors in the test results. The following analysis shows the dielectric permittivity test results of multiple measurements for different parts of the same sample.

4.1.1. Real Part of Dielectric Permittivity. Figure 3 showed the results of the real part of the dielectric permittivity test for the sample with 18.58% mass water content and 1.73 g/cm^3 dry density. The 10 repetitions of the dielectric permittivity real part test show the same characteristics of changing with frequency, which decreases rapidly with the increase of frequency in the low-frequency band, and the real part value of the dielectric permittivity is basically unchanged after the frequency is about greater than 200 MHz.

Taking the results of multiple tests of the real part of the dielectric permittivity at 900 MHz as an example, the values of the 10 measurements varied in the range of 20.03 to 23.65, with a mean value of 21.86 and a standard deviation of 0.93 (Figure 4), indicating that the results of the multiple tests of the real part of the dielectric permittivity were in high agreement, the samples were in good isotropic agreement, the instrument has high testing accuracy and can better present the characteristics of the dielectric permittivity of the samples.

4.1.2. Imaginary Part of Dielectric Permittivity. Again, taking sample #5 with a mass water content of 18.58% and a dry density of 1.73 g/cm^3 as an example, Figure 5 showed the imaginary part of its dielectric constant test results. The results of the 10 repetitions of the dielectric permittivity real part test show highly consistent characteristics of changing with frequency, which decreases rapidly with increasing frequency in the low frequency band, and the value of the imaginary part of the dielectric permittivity is basically unchanged after the frequency is about greater than 400 MHz.

Taking the results of multiple tests of the imaginary part of the dielectric permittivity at 900 MHz as an example, Figure 6 showed the values of the 10 measurements varied in the range of 2.41 to 3.06, with a mean value of 2.73 and a standard deviation of 0.15, indicating that the results of the multiple tests of the imaginary part of the dielectric permittivity were in high agreement, the samples were in good isotropic agreement, the instrument has high testing accuracy on the dielectric permittivity imaginary part.

4.1.3. Tangent of Loss Angular. Again, taking the sample with 18.58% mass water content and 1.73 g/cm^3 dry density as an example, Figure 7 showed the variation of its loss angular tangent with frequency can be obtained according to the test of its dielectric permittivity real part and imaginary part. The variation of the loss angle tangent with frequency obtained from 10 repeated measurements is basically the same, which decreases rapidly with increasing frequency in the low frequency band, and the imaginary part value of the dielectric permittivity is basically unchanged after the frequency is about higher than 400 MHz.

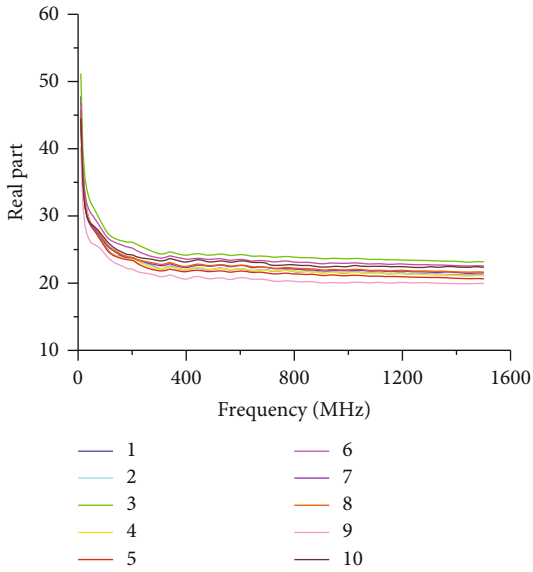

Figure 3: The real part of sample #5 dielectric permittivity changing with frequency under 10 repeated measurements.

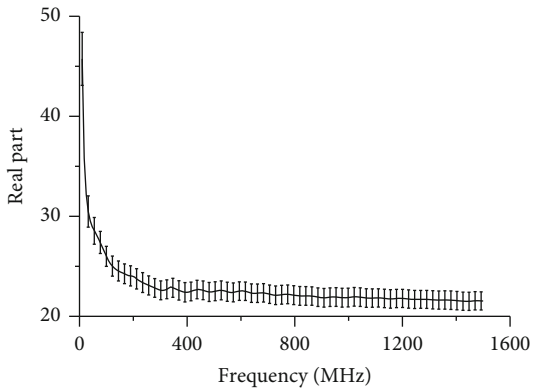

Figure 4: The real part statistical characteristic of sample #5 dielectric permittivity under different frequency

Figure 8 showed the tangent of loss angular statistical characteristic error under different frequency. The value of 10 measurements varies from 0.12 to 0.13 with a mean value of 0.12 and a standard deviation of 0.003 (results of multiple tests of dielectric permittivity imaginary part at 900 MHz, which indicates that the loss angular tangent of different parts is consistent, and the instrument has high accuracy in testing the loss angular tangent of the sample.

4.2. Repeated Tests of Samples of the Same Water Content and Compaction. To reduce the error during the preparation of the remodeled samples, two samples were prepared for the sample of each water content and compaction level for dielectric permittivity tests. The subsequent data processing used the average value of the two samples for each water content and compaction level for analysis.

Taking the samples with a mass water content of 13.77% and a dry density of 1.91 g/cm^3 as an example, Figures 9–11 showed the variation of the real part, imaginary part, and

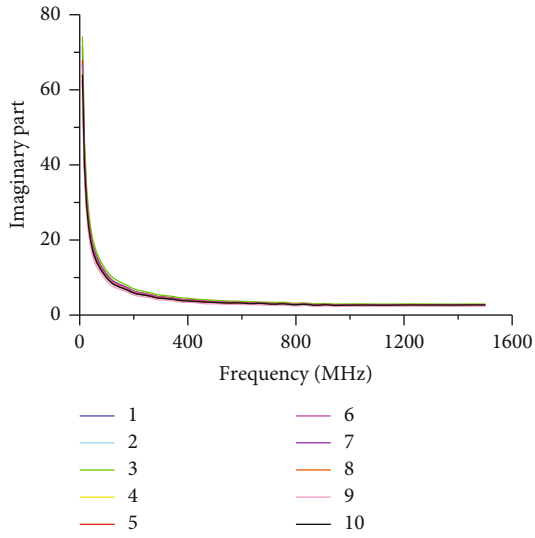

Figure 5: The imaginary part of sample #5 dielectric permittivity changing with frequency under 10 repeated measurements.

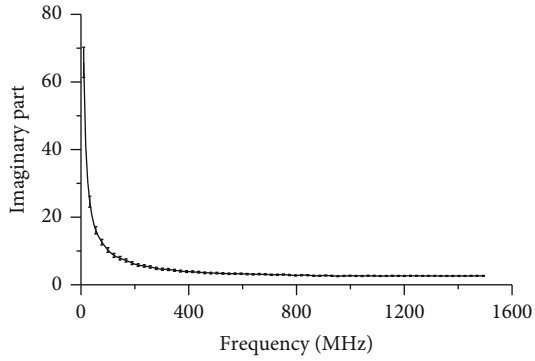

Figure 6: The imaginary part statistical characteristic of sample #5 dielectric permittivity under different frequency.

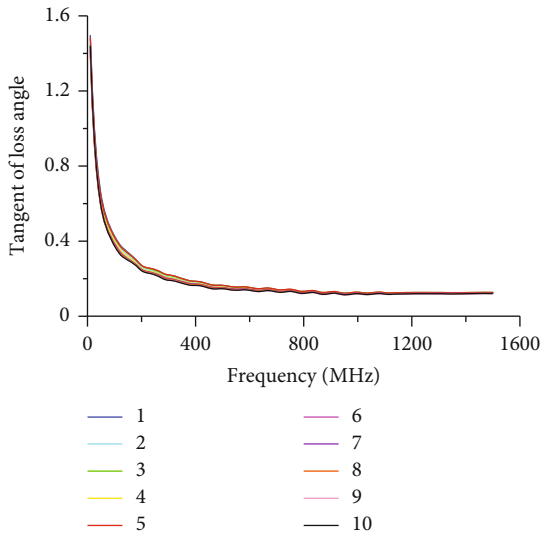

Figure 7: The sample #5 tangent of loss angular changing with frequency under 10 repeated measurements.

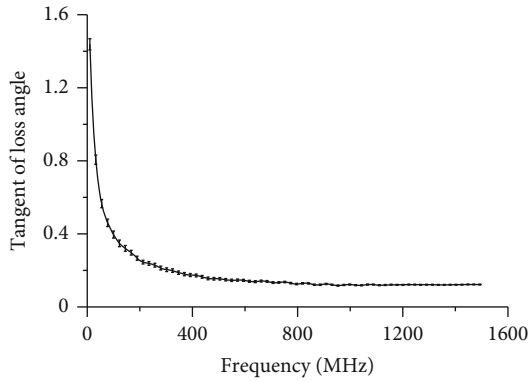

Figure 8: The sample #5 tangent of loss angular error statistical characteristic under different frequency.

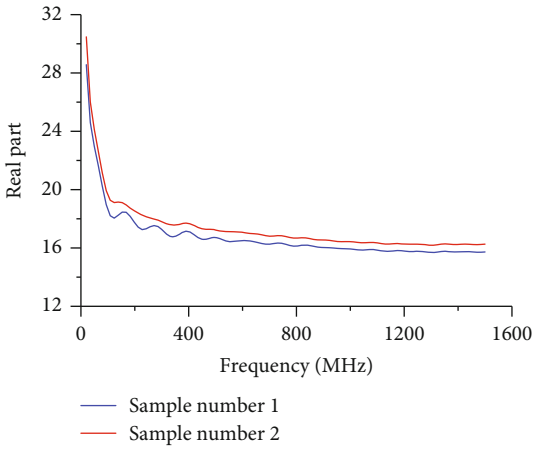

Figure 9: The real part of dielectric permittivity of samples changing with the same water content and compaction level under different frequency.

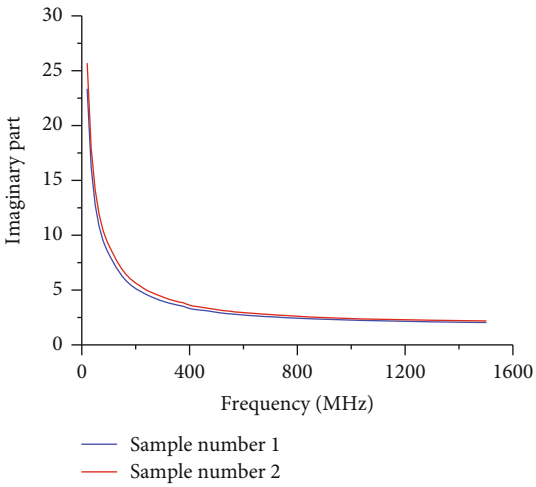

Figure 10: The imaginary part of dielectric permittivity of samples changing with the same water content and compaction level under different frequency.

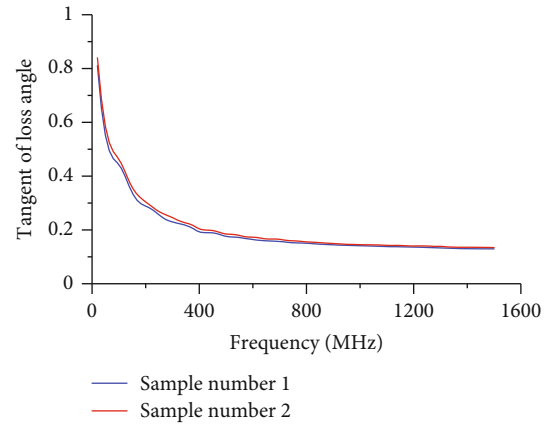

Figure 11: The tangent of loss angular of samples changing with the same water content and compaction level under different frequency.

loss angular tangent of the dielectric permittivity with frequency for the two samples. The variation of the real part of dielectric permittivity, imaginary part and loss angle tangent with frequency show similar characteristics. At 900 MHz, the real parts of the dielectric permittivity are 16.03 and 16.54, respectively, the imaginary parts of dielectric permittivity are 2.33 and 2.48, respectively, and the loss angular tangents are 0.14 and 0.15, respectively. The errors of the real part, imaginary part, and loss angular tangent of the dielectric permittivity of both samples are minor, which indicates that the preparation of different experimental samples and the dielectric permittivity test has good repeatability, and the data accuracy and reliability are high.

4.3. Characteristics of Dielectric Permittivity of Samples with Different Water Content and Compaction Level

4.3.1. Effects of Water Content Variation on dielectric permittivity for Samples of the Same Compaction level. Figure 12 showed the water content variation and dielectric permittivity relationship for samples of the same compaction level. Both the water content and compaction level have effects on the sample dielectric permittivity at the same time. The sample dielectric permittivity increases as the water content increases and is linearly correlated. The values of dielectric permittivity of samples with close or the same water content increases as the compaction level increases.

The fitted trend lines of the dielectric permittivity values variation with water content for samples of the same compaction level show that the effect of the water content variation on the dielectric permittivity is more significant for the samples with high compaction levels, while the effect of the water content variation on the dielectric permittivity values is less significant for the samples with low compactions levels.

4.3.2. Dielectric Permittivity Variation of Samples with the Same Water Content and the Different Compaction levels. Figure 13 showed the dielectric permittivity values of samples with different compaction levels and the same water content, the variation gradient of dielectric permittivity values with increasing dry density for the sample with 20.0% water

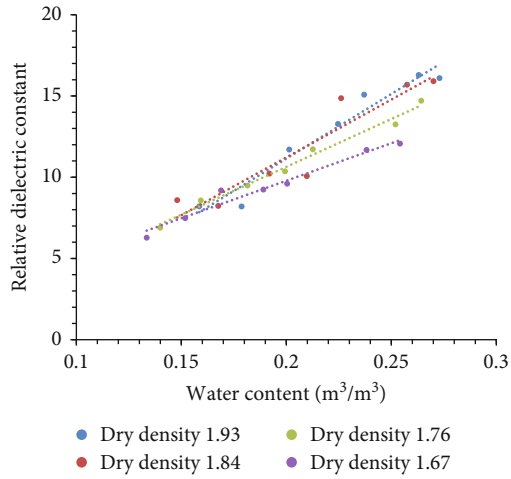

Figure 12: The dielectric permittivity values relationship of samples changing with the same compaction level and different water contents under different frequency

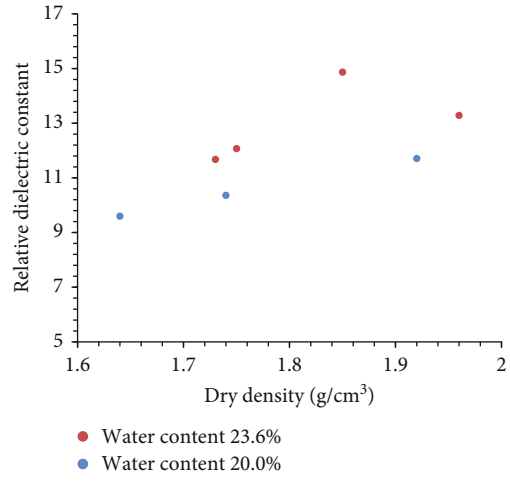

Figure 13: The relative dielectric permittivity values of samples changing with different compaction levels and the same water content under different frequency.

content is lower than that for the sample with 23.6% water content. At lower water content, the sensitivity of the dielectric permittivity to the change of compaction level is low, and the values of dielectric permittivity of samples with different compaction levels were close to each other; the reason is that, at lower water content, although the sample compaction level increases, the change of internal pore water connectivity and free water content are not apparent, and thus the dielectric permittivity variation is not obvious; when the water content is larger, the increase of compaction level will significant increase the pore water connectivity, and thus the compaction level has a great influence on the dielectric permittivity value.

5. Relational Models of the Dielectric Permittivity and Water Content

Different relational models describing the relationship between water content and dielectric permittivity have been developed in existing studies, and different relational models are applicable to different conditions:

Debye Equation: good approximation of the dielectric permittivity for pure or dilute polarized liquids, but not applicable for more complex polarized substances such as solvents and molecular mixtures

Cole and Cole Model: suitable for simulating the effective dielectric permittivity characteristics of water and some simple substances, but performs generally for more complex mixtures such as soils and rocks

Annan (Topp Equation): within the frequency range of ground-penetrating radar (10 MHz-1GHz), the water content in the soil is good in the range of 5%-50%, and its accuracy can be improved by analyzing the experimental data to derive polynomial coefficients (the solid material is assumed to have low loss, and the dielectric permittivity in the dry state is 3-4)

The complex refractive index model (CRIM): suitable for medium to coarse grains, simple particles (e.g. semicircular sand grains), multiphase mixtures and medium to low viscosity fluids, with low estimation of the loss below 100 MHz

BHS Model: similar to the CRIM Model, considering different geometries of particles

The most used form of TOPP Equation is

$$\theta = -5.3 \times 10^{2} + 2.92 \times 10^{-2}\varepsilon - 5.3 \times 10^{-4}\varepsilon^{2} + 4.3 \times 10^{-6}\varepsilon^{3}. \quad (1)$$

where the θ is the volumetric water content, ε is the dielectric permittivity.

To improve the accuracy of the TOPP Equation on the fitting relationship between the dielectric permittivity and water content, the polynomial coefficients of the TOPP Equation need to be corrected based on different soil types and different application conditions. In this study, based on the results of dielectric permittivity tests on samples with different water contents and different compaction levels in the table, the relationship between dielectric permittivity and soil volumetric water content was fitted by applying cubic polynomials, and the fitting relational equation for medium and coarse sandy soils under compacted condition was obtained as

$$\theta = 4 \times 10^{-3} + 1.9 \times 10^{-2}\varepsilon + 3 \times 10^{-4}\varepsilon^{2} - 3 \times 10^{-5}\varepsilon^{3}. \quad (2)$$

The R^2 value for the equation fit was 0.9001, indicating a good fit of this relational model (Figure 14).

The Figure 15 showed the fitted relative errors of samples with different volume water contents in the application of the fitting relational model in Equations (2). It can be seen that the relative errors of the fitting equation for samples with different water contents are within ±10% (Figures 3–13), and the absolute error is ±0.03 m^3/m^3 (Figure 16).

Since the CRIM Model considers the volumetric proportions of the different components in the soil, as well as the relative dielectric permittivity values of each component, and the porosity characteristics, the effect of different

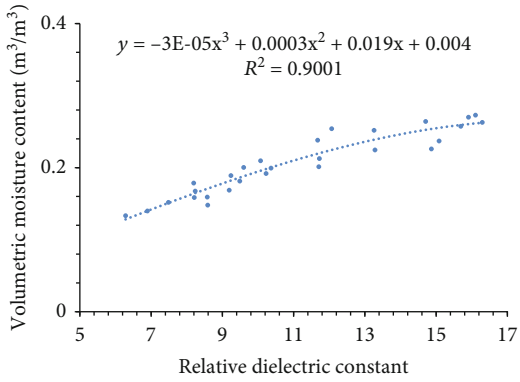

Figure 14: The fitting relationship between relative dielectric permittivity and volumetric water content of sample.

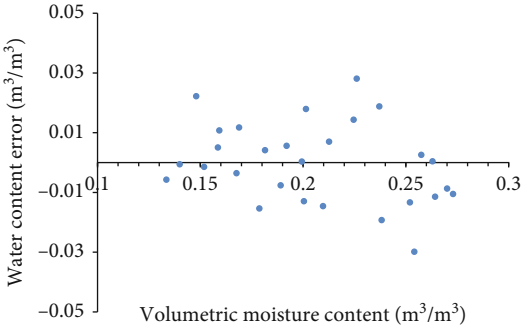

Figure 15: The relative errors between calculated water contents and measured water contents by the fitting relational formula.

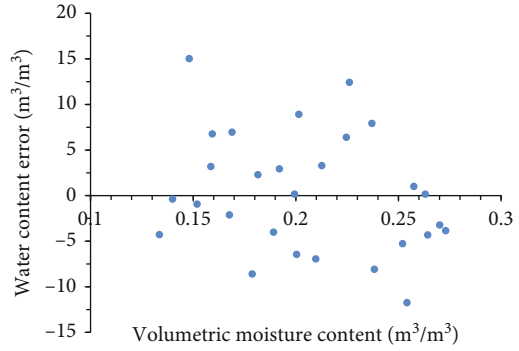

Figure 16: The absolute errors between calculated water contents and measured water contents by the fitting relational formula.

compaction levels on the dielectric permittivity of the soil mixture can be studied based on the relationship between the porosity, the dielectric permittivity values of each component, and the dielectric permittivity values of the soil mixture as follows:

$$n = \frac{\theta\left(\sqrt{\varepsilon_a} - \sqrt{\varepsilon_w}\right) - \sqrt{\varepsilon_s} + \sqrt{\varepsilon_{eff}}}{\sqrt{\varepsilon_a} - \sqrt{\varepsilon_s}}, \quad (3)$$

where the n is the soil porosity, θ is the volumetric water content, $\varepsilon_a, \varepsilon_w, \varepsilon_s$, and ε_{eff} are the dielectric permittivity of

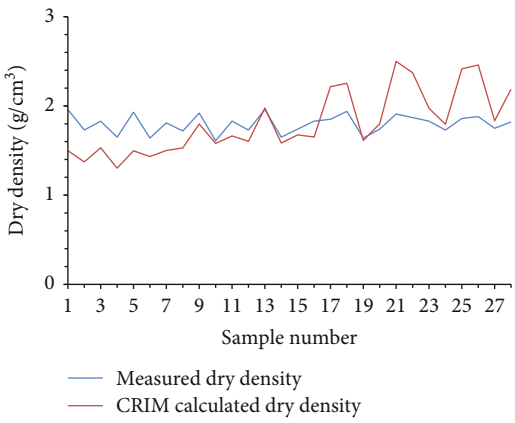

Figure 17: The measured soil sample dry density and predicted dry density by the complex refractive index model (CRIM).

air, free water, solid phase, and soil mixture, respectively, and the relationship between dry density and porosity is as follows:

$$\rho_d = 2.65 \times (1 - n), \quad (4)$$

where the is the dry density of soil, n is the soil porosity.

thus, the dry density characteristics of the soil can be obtained from the dielectric permittivity test.

Figure 17 showed the characteristics of the measured dry density and the calculated dry density of the soil based on the dielectric permittivity test. From Figures 4 and 5, when the water content was low, the measured dry density of the samples and the calculated dry density have a basically same variation trend, while there was a certain error between the two, the measured values of samples 9-15 were more consistent with the calculated values, and as the water content of the samples increases, the calculated values start to be significantly larger than the measured values.

The larger error of the higher water content samples may be due to the unsaturated soil conditions considered in the CRIM Model for calculating porosity, while the compacted soil samples with higher water contents were close to saturation, and the applied unsaturated relational model brought certain errors. Other factors were the dielectric permittivity test error, and the difference between free water and bound water were not considered in the CRIM Model. The dielectric permittivity value of bound water was significantly lower than that of free water due to the surface force of solid particles, thus introducing some errors to the model.

6. Conclusions

(1) In the sample dielectric permittivity test study, it was found that the water content and the density had an effect on the sample dielectric permittivity at the same time. The dielectric permittivity increased as water content increased, and for samples with similar or identical water contents, the value of dielectric permittivity increased as compaction level increased; for samples with high compaction levels, the effect of

water content variation on dielectric permittivity was more significant, while for samples with low compaction levels, the effect of water content variation on dielectric permittivity value was less significant. In view of this, the state of water content distribution can be evaluated by the characteristics of the dielectric permittivity variation, and then the condition of the compaction level characteristics

(2) The dielectric permittivity characteristics of the samples can be evaluated based on their compaction levels. At low water content, the sensitivity of the dielectric permittivity to the compaction level variation was low, and the dielectric permittivity values of samples with different compaction levels were close to each other; the reason was that, at low water content, although the sample compaction level increased, the change of internal pore water connectivity and free water content was not significant, and therefore the change of dielectric permittivity was not obvious; while when the water content was large, the increase of compaction level will significantly increase the pore water connectivity, and therefore having large effects on dielectric permittivity values

(3) The TOPP Equation and CRIM Model were applied to fit the characteristics of the sample such as the dielectric permittivity, water content, and porosity, and the parameters of the TOPP Equation were corrected according to the experimental data to establish the relationship between dielectric permittivity and soil water content of sandy soils under compaction. The joint TOPP Equation and CRIM Model can calculate the characteristics of soil compaction level. When the water content was low and increased to the optimum water content, the measured dry density and the calculated dry density of the sample have a basically same variation trend, and the measured and calculated values were basically the same near the optimum water content; with the further increase of water content to the saturated state of the soil, the calculated values start to be significantly larger than the measured values, and there exist a certain error between the two values

(4) The large errors in the samples with high water contents might be due to the unsaturated soil conditions considered in the CRIM Model for calculating porosity, while the compacted soil samples with high water content were close to saturation, and the application of unsaturated relational model brought some errors. Besides, the dielectric permittivity test errors and the differences between free water and bound water were not considered in the CRIM Model might be the main reasons for the errors in the calculation of the compaction level

(5) Through the test fitting of different soil compaction levels, the parameters of TOPP Equation were corrected, and the joint corrected TOPP Equation and CRIM Model can calculate the empirical relationship of soil compaction level will provide an important basis for the study of water content and compaction level of highway subgrade soil by geological radar method

Data Availability

The data used to support the findings of this study are included within the article.

Conflicts of Interest

The authors declare that they have no conflicts of interests.

Acknowledgments

This study was supported by the Science and Technology Project of Gansu Department of Transportation (Grant No. 2019-18).

References

[1] H. B. Lv, J. W. Yu, Z. Y. Lin, and Z. T. Zeng, "Relationship between volume moisture content and equivalent dielectric constant of Nanning expansive soil," *Rock and Soil Mechanics*, vol. 37, no. 8, pp. 2145–2150, 2016.

[2] L. Y. Li, L. X. Zhang, and S. J. Zhao, "Study on dielectric constant of frozen soil," *Journal of Beijing Normal University (Natural Science Edition)*, vol. 43, no. 3, pp. 241–244, 2007.

[3] M. D. Deshpande, C. J. Reddy, P. I. Tiemsin, and R. Cravey, "A new approach to estimate complex permittivity of dielectric materials at microwave frequencies using waveguide measurements," *Microwave Theory and Techniques, IEEE Transactions on*, vol. 45, no. 3, pp. 359–366, 1997.

[4] X. Y. Kang, L. Lin, Y. J. Liu, and L. S. Shi, "Study on soil dielectric constant water content relationship model," *Rural water conservancy and hydropower in China*, vol. 8, pp. 8–12, 2015.

[5] Z. Zhou, G. Li, M. Shen, and Q. Wang, "Dynamic responses of frozen subgrade soil exposed to freeze-thaw cycles," *Soil Dynamics and Earthquake Engineering*, vol. 152, article 107010, 2022.

[6] Z. Zhou, W. Ma, S. Zhang, Y. Mu, and G. Li, "Effect of freeze-thaw cycles in mechanical behaviors of frozen loess," *Cold Regions Science and Technology*, vol. 146, pp. 9–18, 2018.

[7] J. Teng, J. Liu, S. Zhang, and D. Sheng, "Frost heave in coarse-grained soils: experimental evidence and numerical modelling," *Géotechnique*, pp. 1–12, 2022.

[8] J. Teng, H. Yan, S. Liang, S. Zhang, and D. Sheng, "Generalising the Kozeny-Carman equation to frozen soils," *Journal of Hydrology*, vol. 594, article 125885, 2021.

[9] M. Bittelli, M. Flury, and K. Roth, "Use of dielectric spectroscopy to estimate ice content in frozen porous media," *Water Resources Research*, vol. 40, no. 4, p. W04212, 2004.

[10] D. Robinson, S. Jones, J. Wraith, D. Or, and S. Friedman, "A review of advances in dielectric and electrical conductivity measurement in soils using time domain reflectometry," *Vadose Zone Journal*, vol. 2, no. 4, pp. 444–475, 2003.

[11] J. J. Qing, *Study on the relationship between soil dielectric parameters and moisture content and compactness and its*

engineering application, [M.S. thesis], Xi'an University of technology, Xian, China, 2014.

[12] H. He and M. Dyck, "Application of multiphase dielectric mixing models for understanding the effective dielectric permittivity of frozen soils," *Vadose Zone Journal*, vol. 12, no. 1, p. 22, 2013.

[13] G. Olhoeft, "Electrical properties from 10-3 to 10+9 HZ–physics and chemistry," in *AIP Conference Proceedings*, vol. 154, p. 291, AIP Publishing, 1987.

[14] G. Topp, J. Davis, and A. P. Annan, "Electromagnetic determination of soil water content: measurements in coaxial transmission lines," *Water Resources Research*, vol. 16, no. 3, pp. 574–582, 1980.

[15] M. C. Dobson, F. T. Ulaby, M. T. Hallikainen, and M. A. El-Rayes, "Microwave dielectric behavior of wet soil-part ii: dielectric mixing models," *Geoscience and Remote Sensing, IEEE Transactions on Geoscience and Remote Sensing*, vol. -GE-23, no. 1, pp. 35–46, 1985.

[16] K. Roth, R. Schulin, H. Flühler, and W. Attinger, "Calibration of time domain reflectometry for water content measurement using a composite dielectric approach," *Water Resources Research*, vol. 26, no. 10, pp. 2267–2273, 1990.

[17] U. Wollschlager, H. Gerhards, Q. Yu, and K. Roth, "Multichannel ground-penetrating radar to explore spatial variations in thaw depth and moisture content in the active layer of a permafrost site," *The Cryosphere*, vol. 4, no. 3, pp. 269–283, 2010.

[18] C. M. Steelman and A. L. Endres, "Assessing vertical soil moisture dynamics using multi-frequency GPR common- midpoint soundings," *Journal of Hydrology*, vol. 436-437, pp. 51–66, 2012.

[19] C. M. Steelman, A. L. Endres, and J. P. Jones, "High-resolution ground-penetrating radar monitoring of soil moisture dynamics: field results, interpretation, and comparison with unsaturated flow model," *Water Resources Research*, vol. 48, no. 9, 2012.